Nanogap Detector Inside Nanofluidic Channel for Fast Real-Time Label-Free DNA Analysis

Xiaogan Liang and Stephen Y. Chou*

NanoStructure Laboratory, Department of Electrical Engineering, Princeton University, Princeton, New Jersey 08544

ABSTRACT

We report fabrication and characterization of a novel real-time, label-free DNA detector, that uses a long nanofluidic channel to stretch a DNA strand and a nanogap detector (with a gap as small as 9 nm) inside the channel to measure the electrical conduction perpendicular to the DNA backbone as it moves through the gap. We have observed electrical signals caused by 1.1 kilobase-pair (kbp) double-stranded (ds)-DNA passing through the gap in the nanogap detectors with a gap equal to or less than 13 nm.

Ultrafast, real-time, label-free analysis (e.g., sequencing) of an individual DNA is of great importance to many areas of biology and medicine.[1–3] One primary approach today is the nanopore detectors, which detect the properties of an individual DNA strand real-time by pulling the strand through a pore while measuring the changes in the ionic current through the pore caused by the DNA blockage.[4–7] However, to potentially detect a single base of DNA, the current nanopore detectors must overcome two challenges. The first challenge is the random motion of DNA in solution due to poor confinement of a DNA strand in a nanopore. Nanopore confines only a tiny portion of a DNA strand inside the pore (e.g., in a 3.4 nm long pore, only ∼0.1% of a 10 kilobase (kb) DNA is confined), most of the DNA strand is unrestrained and thus is free to rapidly wiggle around, fold, or tangle. This random motion creates a large amount of noise in the ionic current measurement, which could obscure the signal from a single base. Furthermore, this random motion also makes it hard to control the speed of DNA passing through the pore. The second challenge to nanopores is the signal sensitivity, even if a DNA strand is restrained and stabilized. The nanopore detector measures the DNA blockage of ionic current through a nanopore, which is an electrical signal along the DNA backbone, that depends on both the DNA bases inside the nanopore as well as some DNA bases outside the nanopore. It is still to be seen whether such detection is sensitive enough to resolve two adjacent DNA bases.

Here, we report fabrication and characterization of a real-time, label-free DNA detector, that uses a long nanofluidic channel to stretch a DNA strand into a linear chain, while
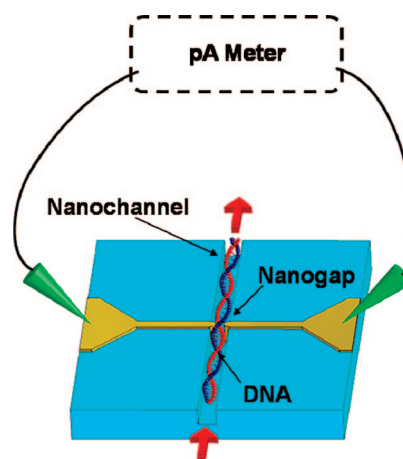

Figure 1. Schematic of a DNA detector with a nanogap inside a nanofluidic channel. The detector uses a long nanofluidic channel to stretch a DNA strand into a linear chain, while using a nanogap detector, consisting of a pair of metal nanowires with a gap (as small as 9 nm), to measure electrical conduction perpendicular to the backbone of a DNA strand as it passes through the gap.

using a nanogap detector, consisting of a pair of metal nanowires with a gap as small as 9 nm, to measure the electrical conduction perpendicular to the DNA backbone as it passes through the gap (Figure 1). A nanogap detector is expected to overcome the challenges in nanopore detectors, because it has been demonstrated that a long narrow nanochannel is very effective in linearizing a DNA;[8–17] a centimeter long, 11 nm wide single fluidic channel with uniform width can be fabricated;[18] and ultrasmall and ultrasensitive electronic detectors also can be fabricated.[19–23] Furthermore, theoretical study suggests that a tunneling
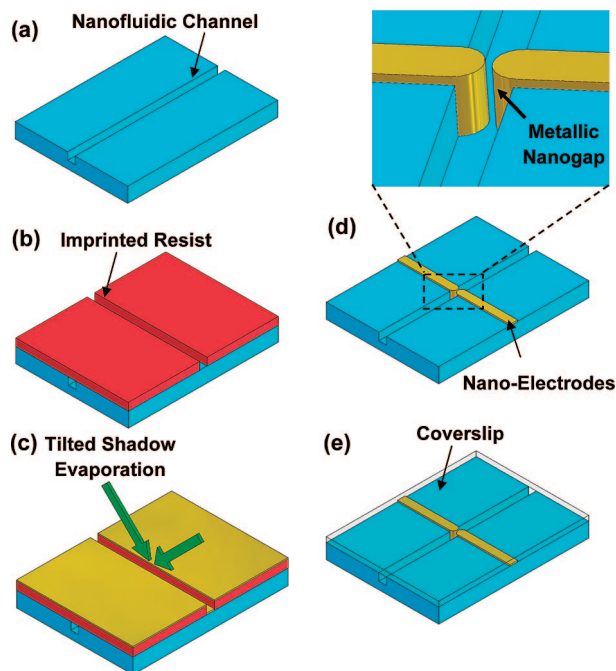
* Corresponding author. E-mail: chou@princeton.edu.

Figure 2. Key steps in the fabrication of nanogap detectors. (a) Fabrication of a single nanofluidic channel on a fussed-quartz substrate; (b) imprinting of a nanotrench into the resist layer, which is perpendicularly across the nanochannel, for a subsequent mental lift-off; (c) deposition of the metals in the nanotrench via the shadow evaporation with two symmetric tilted angles; (d) after a lift-off, a pair of metallic nanowires is formed across the nanochannel with a sub-10 nm breaking gap in the channel (see inset); and (e) after making final metal contacts, the nanochannel, nanowire, and nanogap are conformably sealed by a coverslip coated with a conformable layer.

current perpendicular to a DNA backbone is very sensitive to a single base type of a DNA.[24,25]

The nanogap detectors were fabricated on a fused silica substrate by using two nanoimprint steps (first a nanofluidic channel, and second a metallic nanowire pair with a nanogap inside the channel), etching, metal shadow evaporations, and sealing. The mold used for the nanochannel fabrication was fabricated by anisotropic wet etching of crystalline silicon, conformal deposition of mold material, and anisotropic reactive ion etching (RIE).[18] The mold for making metallic nanowires was patterned by electron-beam lithography (EBL). The key steps in the nanogap device fabrication (Figure 2) include (a) fabrication of a single nanofluidic channel on a fused silica substrate using nanoimprint lithography and RIE[18] (in this step, H-shape microinlet and outlet were also fabricated using photolithography and RIE, and accessing holes were drilled);[13,26] (b) fabrication of a narrow trench in resist using nanoimprint aligned normal to the nanochannel for a subsequent lift-off of metals to form the metallic nanowires and the nanogap; (c) after removing the resist residual layer left by nanoimprint, fabrication of a metal nanowire pair with a nanogap inside the nanochannel by using double shadow evaporations of metal and a lift-off in a solvent (the method makes the nanogap precisely self-aligned inside the nanochannel, and narrows the DNA passage at the gap region); and (d) fabrication of metal contacts to the nanowires; and (e) sealing of the top of the nanochannel by pressing a thin Pyrex
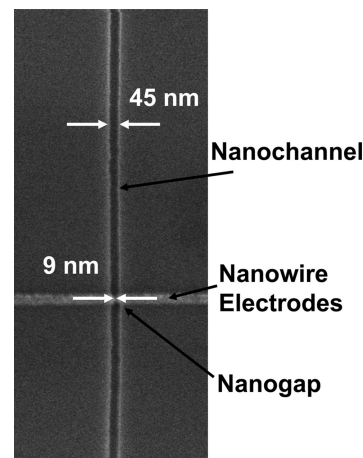
Figure 3. Top-view scanning electron micrograph of a nanogap detector without top sealing plate. A typical nanogap detector has a fluidic channel of 50 μm length, 45 nm width, and 45 nm depth, and a pair of metal nanowires of 45 nm width, 18 nm thickness, and different gap sizes and gap-heights that vary from 20 to 9 nm and from 30 to 16 nm, respectively.

glass plate, which was coated with a thin conformable adhesion layer, on top of the substrate. Particularly, we used Nanonex NX-2000 imprintor, Nanonex NXR-3020 resists, and an alignment station for imprint, O_2−plasma for RIE, and a heating at 100 to 110 °C for 0.5 to 2 min for the device sealing. One of the advantages of using nanoimprint is a fast turnaround and high fabrication reliability (yield).[27,28]

Using this process, we have fabricated the nanogap DNA detectors with a fluidic channel of 50 μm length, 45 nm width, and 45 nm depth, and a pair of metal nanowires of 45 nm width, 18 nm thickness (4 nm Ti/14 nm Au), and different gap size and gap height that varies from 20 to 9 nm and from 30 to 16 nm, respectively. The contact pads to the nanowires were 10 nm Ti/80 nm Au. Figure 3 shows the top view scanning electron micrograph of a nanogap detector, before putting on a top cover plate.

The gap of a nanogap detector was controlled by the initial fluidic channel width, the shadow evaporation angle, and the evaporation material thickness. The final height at the nanogap detector was determined by the amount of conformable adhesion material coated on the thin Pyrex glass coverslip that was squeezed into the gap during the sealing. We found that the material squeezed reduces only the height at the nanogap area but not the part of the channel outside the nanogap. Figure 4 shows three different cross sections of nanogap detectors after sealing, which are 9 nm (gap) × 16 nm (height), 13 nm × 26 nm, and 18 nm × 35 nm, respectively.

To test nanogap detectors, 1.1 kilobase-pair (kbp) double-stranded (ds)-DNAs were prepared from Sureslicensing™ shRNA plasmid (SuperArray Bioscience Corp.). The cleavage was performed at two sites with PstI restriction enzyme to produce sticky-end ds-DNAs. The reaction mixture was applied to 0.8% agarose gel and further purified by an agarose gel purification kit (QIAGEN Inc.). The purity of the DNA was finally confirmed by UV absorbance. The prepared DNAs were dissolved at a concentration of 0.5 mg/mL in 0.5 × TBE buffer

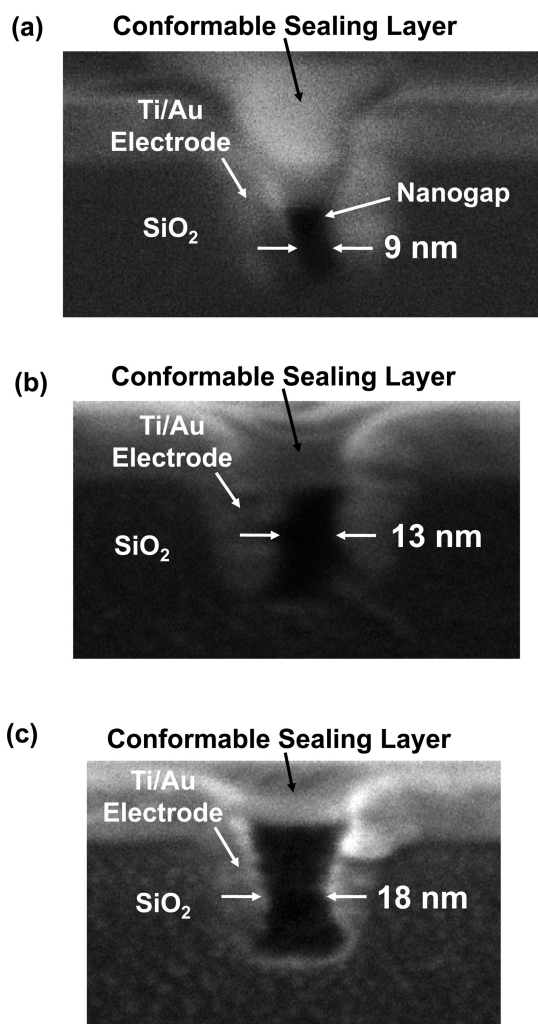**Figure 4.** Scanning electron micrographs of three different cross sections (gap × height) of sealed nanogap detectors. (a) 9 nm (gap) × 16 nm (height), (b) 13 nm × 26 nm, and (c) 18 nm × 35 nm.

(0.045 M tris-base, 1 mM EDTA with 0.045 M boric acid, pH 7.5) and stored at −20 °C. The 1.1 kb ds-DNA has persistent length of ∼50 nm, and it is expected to be stretched, in the channel of 45 nm width and depth, and 50 um length, to ∼70% of its natural length of 374 nm[12].

To prepare nanogap detectors for electrical signal testing, we wetted the whole device in a loading buffer (0.045 M tris-base, 1 mM EDTA with 0.045 M boric acid (0.5 × TBE)). Air bubbles were removed by using a vacuum pump. A 10 mV bias was applied across the gap between the metal nanowire pair for electrical current measurement.

The electrical signal amplification was carried out using an Axopatch-200B pA amplifier (Molecular Devices, Inc.), which has a time resolution of 10 μs at 100 kHz bandwidth and an open-circuit noise level (root-mean-square value) of ∼1 pA for 100 kHz bandwidth and 0.13 pA at 10 kHz bandwidth. The amplified signal was digitized by a Digidata 1440 data acquisition system (Molecular Devices, Inc.) with the minimum spacing of sampling time of 4 μs (250 kHz). The data of the current−time curves were finally stored on a computer.

We used the nanogap detectors with different gap sizes to detect the electrical signal of 1.1 kbp ds-DNA in a 0.5 ×
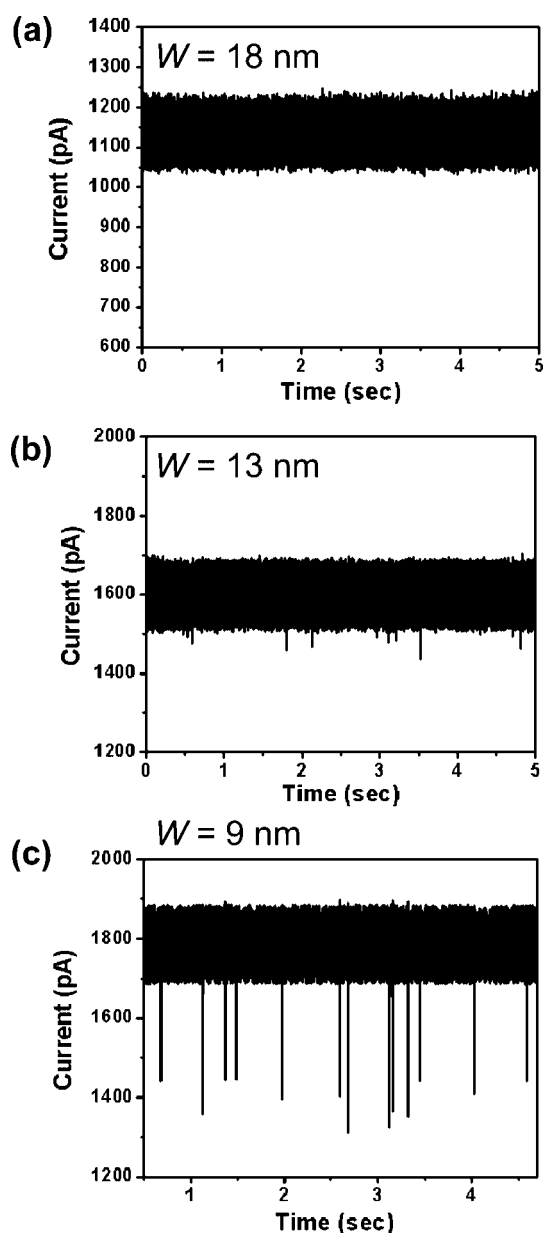

Figure 5. Electrical measurements of DNA in three nanogap detectors with different gap sizes. (a) For cross section of 18 nm (gap) × 35 nm (height), there was no detectable difference in the measured electrical current signals between the pure buffer solution and the buffer solution containing 1.1 kbp of DNA. (The average background current is 1140 pA caused by solvent conductivity, and the noise is ∼50 pA rms due to the ampere meter used.) (b) For 13 nm (gap) × 26 nm (height), clear negative pulses were observed only in the buffer solution containing the 1.1 kbp DNAs but not in the pure buffer solution. And (c) for 9 nm (gap) × 16 nm (height), the average magnitude of negative pulses increases by ∼200% and becomes ∼350 pA.

TBE buffer solution as the DNAs flow in the nanofluidic channel and pass through the nanogap. The DNAs in solution were driven by electrophoresis with Pt electrodes inserted into the liquid reservoirs, which provide an electrophoretic voltage of 20 V. For the nanogap detector with a cross section of 18 nm (gap) × 35 nm (height), there was no detectable difference in the measured electrical current signals between the pure buffer solution and the buffer solution containing 1.1 kbp DNAs (Figure 5a). The detector detected an average
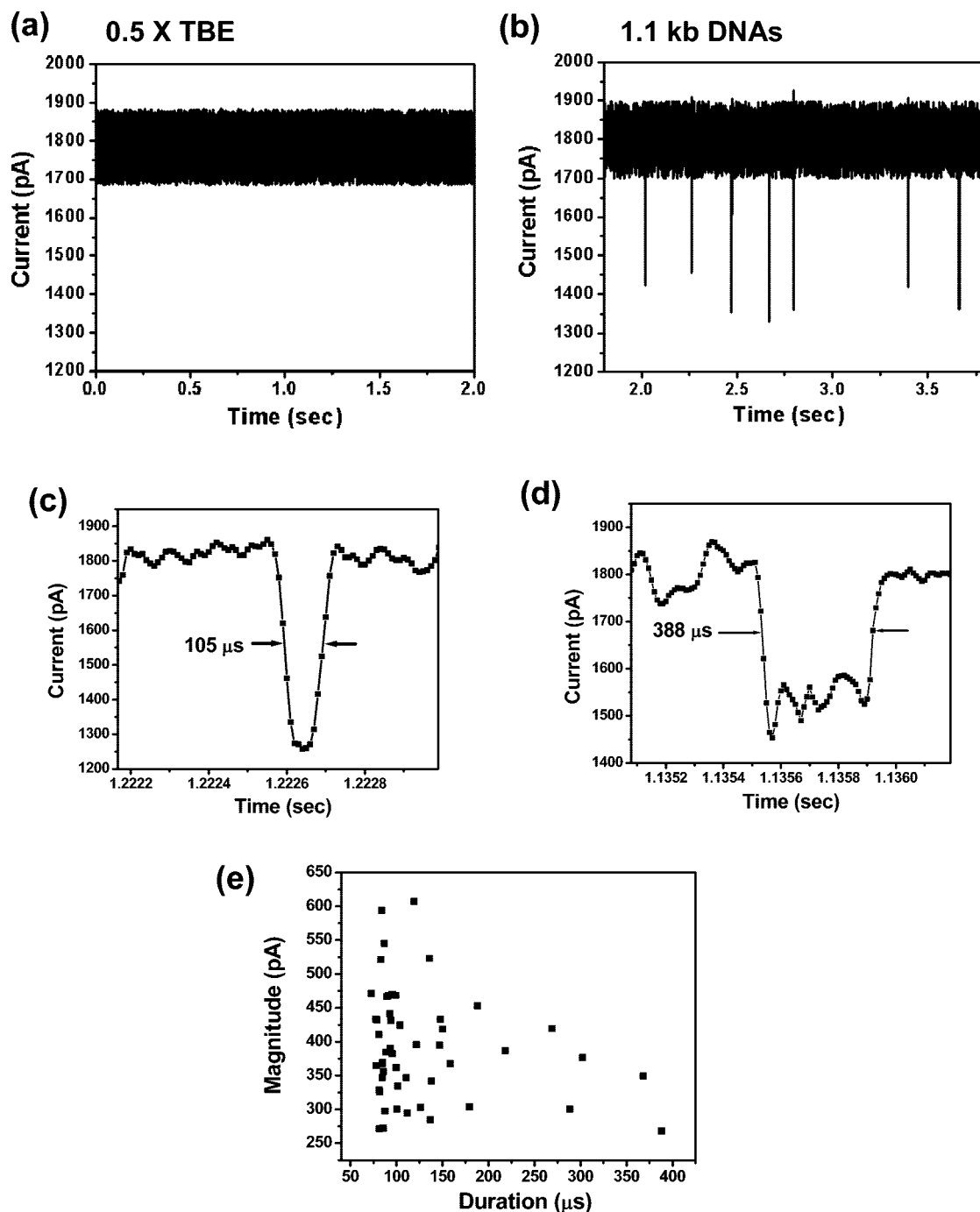
Figure 6. Electrical measurements by a nanogap detector with cross section of 9 nm (gap) × 16 nm (height). (a) No negative pulse train was observed in a pure 0.5 × TBE buffer solution, (b) but the pulse trains were detected when 1.1 kbp ds-DNAs were added into the solution; (c) a signal with a duration of ∼100 μs in an expanded time scale; (d) a signal with a duration of ∼388 μs; and (e) distribution of pulse duration and amplitude of 50 pulses.

current of 1140 pA with a 100 kHz noise of ∼50 pA root-mean-square (rms) magnitude. The current is due to the conductivity of buffer solution, and the noise band is corresponding to the pA meter's close-loop noise at 100 kHz.

However, as the nanogap detector cross section is reduced to 13 nm (gap) × 26 nm (height), clear negative pulses are observed only in the buffer solution containing the 1.1 kbp DNAs but not in the pure buffer solution (Figure 5b). The amplitude of the pulse signals ranges from 100 to 150 pA (noticeably larger than the noise). Furthermore, when the

nanogap cross section is further reduced to 9 nm (gap) × 16 nm (height), the average magnitude of negative pulses increases by ∼200% and becomes ∼350 pA (Figure 5c).

Figure 6 shows further details of the electrical signal measured by a nanogap DNA detector with a nanogap of cross section of 9 nm (gap) × 16 nm (height). The nanogap detectors did not detect any negative pulse trains in a pure 0.5 × TBE buffer solution (Figure 6a) but did detect such signal train in 1.1 kbp ds-DNA solution (Figure 6b). Most of the electrical current pulses have a duration of ∼100 μs

(Figure 6c), but it can be as long as 388 μs (Figure 6d). Given the length of our nanochannels ($L = 50$ μm) and the electrophoretic voltage ($V = 20$ V), the average electric field is 4000 V/cm. If we use the measured electrophoretic mobility for the ds-DNAs in a nanofluidic channel filled with a TBE buffer liquid (very close to our case),[29] $\mu \sim 1 \times 10^{-8}$ m^2/(Vs), the transport velocity of DNAs is estimated to be around $v = \mu V/L \sim 4$ μm/ms. Our measured time duration is reasonable for a 1.1 kb ds-DNA traveling at this estimated speed in the fluidic nanochannel, since it would take, on the basis of the estimated DNA flow speed, 94 μs for a 0.374 μm long DNA to pass through a gap. The distribution of pulse duration is shown in Figure 6e. The negative electrical pulse train disappeared when the electrophoretic voltage that drives DNAs through the fluidic channel was turned off, further indicating that the negative pulse train came from the DNAs passing through the nanogap.

The observations that (a) the negative electrical pulse train appeared only in the solution that contains DNAs not in the pure buffer solution, only with the nanogap of the detector equal to or less than 13 nm but not with the larger gap devices, and only when an electrophoretic voltage for driving DNAs through the channel was on but not when it was off and (b) the pulse duration is consistent with the DNA flow speed and length suggest strongly that the observed signal is caused by a DNA passing through the nanogap detector.

Compared with the background current, the electrical signal caused by a DNA passing through a nanogap shows a reduction in electrical current. This can be explained by the fact that DNA is more insulating than the buffer solution.[30] The observed variation in the electrical signal amplitude may be attributed to the slight variation in the gap size (over the cross section) for a given nanogap detector (see Figure 4). The variation in DNA electrical signal duration can be related to the fact that often the translocation speed of a given length DNA through a given nanochannel is not constant but has a distribution, as being observed by other groups.[31] The variation could be caused by several factors, such as the random friction and local partial clogging experienced by DNAs in the nanochannel or local electric field variation, all of which should be further studied.

However, in our current experiments, we have not resolved the single base of a DNA yet, which is a key goal that we hope to achieve in the future. Currently, the dimensions (in particular, the nanowire width) of our nanogap are large. To improve the detection resolution of nanogap detectors toward single base detection, we need to (a) further reduce the nanogap dimensions (gap, height, and width), (b) reduce the DNA flow speed across the channel, and (c) reduce the fluctuations in DNA translocation time. Undoubtedly, the design, fabrication, and performance in DNA detection of the nanogap DNA detectors presented here lay a good foundation to the development of novel devices for DNA single base detection.

References

(1) Shendure, J.; Mitra, R. D.; Varma, C.; Church, G. M. *Nature Reviews Genetics* **2004**, *5* (5), 335–344.
(2) Chan, E. Y. *Mutation Research-Fundamental And Molecular Mechanisms Of Mutagenesis* **2005**, *573* (1−2), 13–40.
(3) Kricka, L. J.; Park, J. Y.; Li, S. F. Y.; Fortina, P. *Expert Review Of Molecular Diagnostics* **2005**, *5* (4), 549–559.
(4) Li, J.; Stein, D.; McMullan, C.; Branton, D.; Aziz, M. J.; Golovchenko, J. A. *Nature* **2001**, *412* (6843), 166–169.
(5) Li, J. L.; Gershow, M.; Stein, D.; Brandin, E.; Golovchenko, J. A. *Nat. Mater.* **2003**, *2* (9), 611–615.
(6) Li, J. L.; Stein, D.; Qun, C.; Brandin, E.; Huang, A.; Wang, H.; Branton, D.; Golovchenko, J. *Biophys. J.* **2003**, *84* (2), 134A–135A.
(7) Howorka, S.; Cheley, S.; Bayley, H. *Nat. Biotechnol.* **2001**, *19* (7), 636–639.
(8) Austin, R. H.; Brody, J. P.; Cox, E. C.; Duke, T.; Volkmuth, W. *Physics Today* **1997**, *50* (2), 32–38.
(9) Austin, R. H.; Tegenfeldt, J. O.; Cao, H.; Chou, S. Y.; Cox, E. C. *IEEE Transactions On Nanotechnology* **2002**, *1* (1), 12–18.
(10) Jendrejack, R. M.; Schwartz, D. C.; Graham, M. D.; De Pablo, J. J *J. Chem. Phys.* **2003**, *119* (2), 1165–1173.
(11) Reccius, C. H.; Mannion, J. T.; Cross, J. D.; Craighead, H. G. *Phys. Rev. Lett.* **2005**, *95* (26).
(12) Reisner, W.; Morton, K. J.; Riehn, R.; Wang, Y. M.; Yu, Z. N.; Rosen, M.; Sturm, J. C.; Chou, S. Y.; Frey, E.; Austin, R. H. *Phys. Rev. Lett.* **2005**, *94*, 19.
(13) Mannion, J. T.; Reccius, C. H.; Cross, J. D.; Craighead, H. G. *Biophys. J.* **2006**, *90* (12), 4538–4545.
(14) Odijk, T. *J. Chem. Phys.* **2006**, *125* (20), 204904.
(15) Kyubong Jo, D. M. D.; Odijk, T.; de Pablo, J. J.; Graham, M. D.; Runnheim, R.; Forrest, D.; Schwartz, D. C. *Proc. Natl. Acad. Sci. U.S.A.* **2007**, *104* (8), 2673–2678.
(16) Huh, D.; Mills, K. L.; Xiaoyue, Z.; Burns, Mark A.; Thouless, M. D.; Takayama, S. *Nat. Mater.* **2007**, *6* (6), 424–428.
(17) Han, J.; Turner, S. W.; Craighead, H. G. *Phys. Rev. Lett.* **1999**, *83* (8), 1688–1691.
(18) Liang, X. G.; Morton, K. J.; Austin, R. H.; Chou, S. Y. *Nano Lett.* **2007**, *7* (12), 3774–3780.
(19) Guo, L. J.; Leobandung, E.; Chou, S. Y. *Science* **1997**, *275* (5300), 649–651.
(20) Cui, Y. L., C. M. *Science* **2001**, *291* (5505), 851–852.
(21) Austin, M. D.; Ge, H. X.; Wu, W.; Li, M. T.; Yu, Z. N.; Wasserman, D.; Lyon, S. A.; Chou, S. Y *Appl. Phys. Lett.* **2004**, *84* (26), 5299–5301.
(22) Akkerman, H. B.; Blom, P. W. M.; de Leeuw, D. M.; de Boer, B. *Nature* **2006**, *441* (7089), 69–72.
(23) Im, H. S.; Huang, X. J.; Gu, B.; Choi, Y. K. *Nature Nanotechnol.* **2007**, *2* (7), 430–434.
(24) Zwolak, M.; Di Ventra, M. *Nano Lett.* **2005**, *5* (3), 421–424.
(25) Lagerqvist, J.; Zwolak, M.; Di Ventra, M. *Nano Lett.* **2006**, *6* (4), 779–782.
(26) Tegenfeldt, J. O.; Prinz, C.; Cao, H.; Huang, R. L.; Austin, R. H.; Chou, S. Y.; Cox, E. C.; Sturm, J. C. *Anal. Bioanal. Chem.* **2004**, *378* (7), 1678–1692.
(27) Chou, S. Y.; Krauss, P. R.; Renstrom, P. J. *Appl. Phys. Lett.* **1995**, *67* (21), 3114–3116.
(28) Chou, S. Y.; Krauss, P. R.; Renstrom, P. J. *Science* **1996**, *272* (5258), 85–87.
(29) Cross, J. D.; Strychalski, E. A.; Craighead, H. G. *J. Appl. Phys.* **2007**, *102* (2).
(30) de Pablo, P. J.; Moreno-Herrero, F.; Colchero, J.; Gomez-Herrero, J.; Herrero, P.; Baro, A. M.; Ordejon, P.; Soler, J. M.; Artacho, E. *Phys. Rev. Lett.* **2000**, *85* (23), 4992–4995.
(31) Fan, R.; Karnik, R.; Yue, M.; Li, D. Y.; Majumdar, A.; Yang, P. D. *Nano Lett.* **2005**, *5* (9), 1633–1637.

NL080473K